OPEN
Technical note

Nuclear Medicine Communications

Simulation of the distribution of astatine-211 solution dispersion in a lab room

Hitoshi Kubo[a,b], Kazuhiro Takahashi[b], Saki Shimoyama[b], Songji Zhao[b], Naoyuki Ukon[b] and Hiroshi Ito[b,c]

Objective **This study aimed to evaluate the distribution of Astatine-211 (^{211}At) solution dispersion in a small animal cage using autoradiography imaging to simulate the dispersion of ^{211}At in a lab room to eventually prevent user's risk of internal exposure in terms of radiation safety.**

Methods **^{211}At radiation sources with two chemical properties (Na^{211}At and Free ^{211}At) were prepared. The solutions of ^{211}At were placed onto a dish with paper, and then, it was placed in a small animal cage for 3 h. After removing the dish, an imaging plate with attaching reference sources was placed at four walls of the cage for 15 h in a lead box. Imaging plates were read, and all pixel data were calculated using Microsoft Excel 2016 to obtain three-dimensional (3D) distribution. Calculated results were depicted using a 3D sphere model.**

Results **The mean activity of Free ^{211}At was 2.3 times higher than that of Na^{211}At on all autoradiography images. In the cage, the shape of the dispersion of Na^{211}At was almost homogeneous, whereas that of Free ^{211}At was more heterogeneous.**

Conclusion **We found that the solution of ^{211}At vaporized naturally and was distributed heterogeneously in the cage, and the chemical properties of ^{211}At influenced their behaviors. These results must be considered to minimize the risks of radiation safety.** ***Nucl Med Commun*** **42: 1052–1059 Copyright © 2021 The Author(s). Published by Wolters Kluwer Health, Inc.**

Nuclear Medicine Communications 2021, **42**:1052–1059

Keywords: astatine-211, autoradiography imaging, distribution of solution dispersion, radiation safety

[a]Department of Radiological Sciences, School of Health Sciences, [b]Advanced Clinical Research Center and [c]Department of Radiology and Nuclear Medicine, Fukushima Medical University, Fukushima, Japan

Correspondence to Hitoshi Kubo, PhD, Department of Radiological Sciences, School of Health Sciences, Fukushima Medical University, 10-6 Sakaemachi, Fukushima, Fukushima 960 8516, Japan
Tel and fax: +81 24 581 5577; e-mail: kubo-h@fmu.ac.jp

Received 23 December 2020 **Accepted** 23 March 2021

Introduction

Astatine-211 (^{211}At) is one of the useful α-emitting radioisotopes for targeted cancer therapy, and the traces to be used as theragnostic with this radionuclide have been developed globally [1–3]. ^{211}At belongs to halogens and shows some chemical characteristics similar to that of iodine such as volatility and water solubility. It is widely known to people who produce and synthesize radiopharmaceutical agents so that iodine may vaporize well in the process. Inhalation or direct contact with iodine gases must be avoided to minimize the risks of contamination and internal exposure. In terms of chemical characteristics, ^{211}At is considered to have a risk to vaporize well in the process, too. ^{211}At has no stable isotopes, and its half-life is 7.2 h. Because it has no stable isotope, the tracer with ^{211}At has to use ^{211}At itself. Those who handle ^{211}At may be at risk of intake by inhalation or absorption through the skin because of its high volatility.

Evaluating the vaporization and the movement of ^{211}At in the air is challenging because of the low detection capability for α-particle-emitter especially in a large space as a lab room. Some literature referred to the radiation safety of ^{211}At in production, but we could not find any literature referring to this phenomenon as a radiation safety issue [4,5].

Autoradiography imaging is a method of depicting the distribution of radioisotopes tracer using an imaging plate and its reader system. It is used to depict high-resolution images of tracer distribution of the experimental animals such as mice and rats in a preclinical experiment as an ex vivo study. It can detect radioisotopes distribution directly with high sensitivity. Evaluating the radioisotope's distribution of a lab room by directly using this autoradiography system was unrealistic because the imaging plate was not large enough to fit the walls, cell and floor of an actual lab room. The size of the imaging plate was $20 \times 25\,cm^2$, making it suitable for a small animal cage used for the mice and rats. The wind flow in the small animal cage used in an isolated system is regulated to a level comfortable for small animals and is similar to the environment of the radioisotopes lab with an air conditioning system. The small animal cage in the isolation system may be useful in simulating the radioisotopes lab environment and may be useful in depicting radioisotopes solution dispersion directly and quantitatively when combined with an imaging plate. This study aimed

0143-3636 Copyright © 2021 The Author(s). Published by Wolters Kluwer Health, Inc. DOI: 10.1097/MNM.0000000000001430

to evaluate the distribution of ^{211}At solution dispersion in a small animal cage using autoradiography imaging to simulate the dispersion of ^{211}At in a lab room to eventually keep users from the risks of internal exposure.

Materials and methods

Production of ^{211}At

^{211}At was produced through the ^{209}Bi(α,2n)^{211}At reaction using a Sumitomo multipurpose cyclotron (MP-30, Sumitomo Heavy Industries, Ltd., Japan) in the Advanced Clinical Research Center at Fukushima Medical University, Japan. A 30 MeV alpha-particle beam was degraded to 26.5 ± 0.9 MeV by inserting 70 μm of aluminum foil to prevent the production of ^{210}At. The degraded beam was used to bombard the bismuth (99.999%, Goodfellow Cambridge Ltd., Huntingdon, England) layer on an aluminum backing for 110 min with 10.9 eμA. ^{211}At was isolated from the irradiated target using the dry distillation procedure reported by Lindegren *et al.* [6] with slight modifications. Briefly, the target was inserted in a quartz tube placed in a tube furnace preheated to 700 °C. Under helium gas flow in a 700 °C oven, vaporized ^{211}At was transported from the quartz tube to an externally connected PTFE tube that was immersed in a dry ice/ethanol bath. The cooled ^{211}At was trapped in the PTFE tube, eluted and recovered using 0.5 mL of chloroform. The radioactivity of ^{211}At was measured using a dose calibrator (CRC-25R, Capintec Inc., Ramsey, New Jersey, USA), which was previously calibrated by measuring a highly radioactive ^{211}At source using a Ge detector (GEM30-70, ORTEC, Oak Ridge, Tennessee, USA) and a dose calibrator. For the quantification of ^{211}At radioactivity on a Ge detector, we selected 687.0 keV of gamma ray (intensity, Ir = 0.261%) from ^{211}At, and 569.65 keV (Ir = 0.311%, against the decay of ^{211}At) and 897.8 keV (Ir = 0.321%, against the decay of ^{211}At) from the daughter nuclide ^{211}Po. Gamma ray spectrometry was also conducted using a Ge detector to assign the radionuclides produced in the target and the recovery solution of ^{211}At. The radioactivity of ^{211}At was more than 250 MBq at the end of the bombardment, and the radiochemical purity of ^{211}At was more than 99.9% at the end of recovery; there was no contamination of ^{210}At. Chloroform, the recovery solvent of ^{211}At, was added to 50 μL of 0.1 M NaOH aqueous solution and then removed with nitrogen gas. The remaining ^{211}At was redissolved in 3 mL of saline. We call this solution 'Free ^{211}At,' comprising not only ^{211}At(0) but also, to some extent, ^{211}At and several oxidized species such as $^{211}AtO^-$, $^{211}AtO_2^-$, $^{211}AtO_3^-$ and $^{211}AtO_4^-$ [7].

Sodium astatide (Na^{211}At) was prepared as follows. 0.2 mL of Free ^{211}At solution was mixed with 0.5 mL of 2 w/v% sodium ascorbate as a reducing agent and 0.3 w/v% sodium bicarbonate as a pH adjuster. The mixture was stirred for 10 min at ambient temperature. This preparation is a modified previous method [8]. To clarify the ^{211}At solution dispersion behavior with regard to its chemical properties in this study, we developed and compared two chemical solutions of ^{211}At: Na^{211}At and Free ^{211}At. Table 1 shows the chemical species estimated by means of the previous literature. [7–10]

Experimental settings

One Cage Micro-Isolator with RAIR HD One Cage Ventilated Housing System (Lab Products, Inc., Seaford, Delaware, distributed by Natsume Seisakusho Co., Ltd., Tokyo, Japan) was applied as a cage system for small animals. The size of the outside of a cage in this system was 238 mm × 372 mm × 216 mm (W × D × H). CR-35 Bio (Elysia-Raytest, Angleur, Belgium) was applied and used as an imaging plate reader in the autoradiography experiment. In this study, a storage phosphor screen (GE Healthcare, BAS-imaging plate SR2025E) was used as an imaging plate with CR-35 Bio to detect radioactivity. The photostimulable phosphor layer is one layer, sandwiched between the support and protective layers. The protective layer side is coated black to stop the optical transmission. We scanned the opposite side (support layer side) using CR-35 Bio.

ImageJ 1.51j8 (NIH, Bethesda, Maryland, USA) and MicroAVS 12.0 (KGT, Tokyo, Japan) were used for image analyses and three-dimensional (3D) depiction.

The solutions of ^{211}At (adjusted as 111 kBq/200 μL for Free ^{211}At and 109 kBq/200 μL for Na^{211}At) were placed onto 5 cm polyethylene filter paper in a dish. Each dish was placed at the bottom corner of the cage, and there was nothing except the dish in the cage. The cage was placed on a ventilated lack and was left for 3 h (Fig. 1a). After removing each dish, an imaging plate with attaching 500 and 1000 Bq/cm^2 references were placed at the top face, bottom face and both smaller and bigger side faces that were the closest to the dish for 15 h in a lead box (Fig. 1b and c). The reference sources (500 Bq/cm^2 and 1000 Bq/cm^2) were made with 1 cm × 1 cm polyethylene filter paper and wrapped double with a cling film to avoid vaporization. The concentration of the solution to make the reference sources were adjusted from the same one for making the solutions with 5-cm polyethylene filter paper. They were attached to all four imaging plates when exposed. Before attaching the imaging plates to the cage, they were individually wrapped with a cling film to avoid self-contamination and were attached to the outside of the cage. The support layer side was positioned facing the cage.

Image analysis

After finishing each experiment, imaging plates were read by CR-35 Bio with a sensitivity of 25 μm resolution mode and saved to tagged image file format files. Each file was opened on ImageJ and calibrated with the activities of

Table 1 Chemical species of 211At and Na211At

Solution	Speculated chemical species of ^{211}At in water
Free ^{211}At	At^-, At(0), AtO^-, AtO_2^-, AtO_3^-, AtO_4^-
Na^{211}At	At^-

Fig. 1

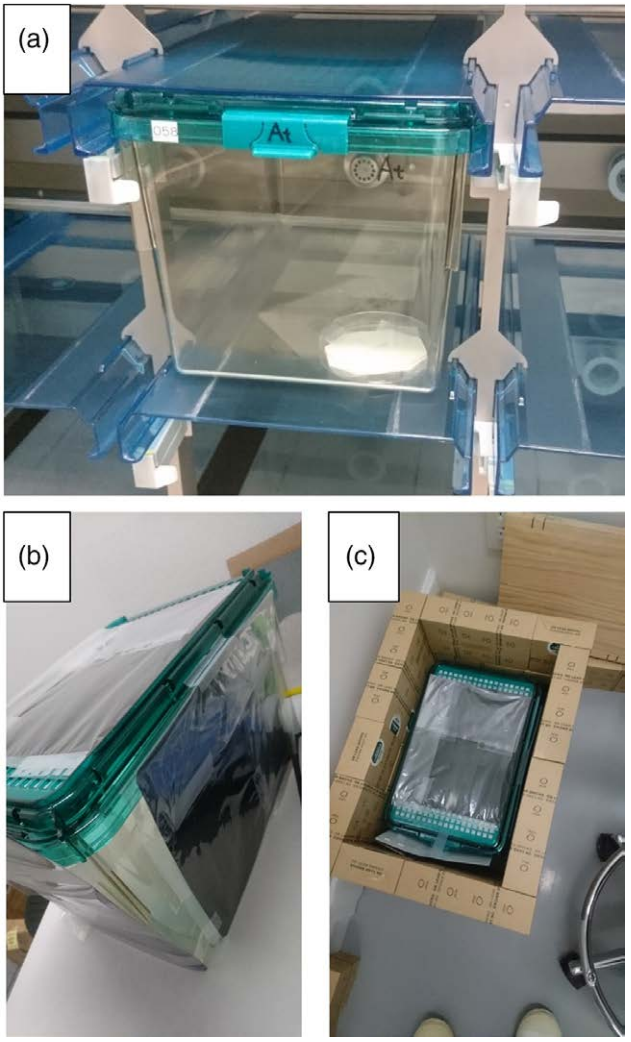

Photos of the settings of our experiments. (a) A cage inserted in the shelf with a dish. (b) imaging plates were attached to the walls of a cage. (c) An imaging plate contacting with imaging plates was placed in a lead box.

two references. The regions of interest (ROIs) were set on the images of the references followed by the reading of their counts. The combinations of the counts and the activities were inputted to the calibration function parameter window of the ImageJ. The pixel values of the images from counts to activities were converted. The shape of the ROIs was a rectangle, with a 1 cm × 1 cm size. After masking the place where two references were set digitally (replacement the pixel values to 0), each result was visualized as a two-dimensional (2D) distribution on four faces with a fixed range, respectively. These results were load in Microsoft Excel 2016, and then, the resolutions of each image were reduced to 20 (width) × 18 (depth) × 15 (height) pixels by pixel averaging.

Three-dimensional results were obtained by correlating the 2D results using Microsoft Excel 2016. Correcting was conducted via the distance weighing method. The pixel value of each position in the inner space of the cage was calculated by linearly weighing from four faces and then normalized with all pixel values. Final calculated results were visualized using MicroAVS as 3D sphere models. Each sphere size and color represents the normalized values of each position.

Results

Figures 2 and 3 respectively show the 2D distribution on four faces of $Na^{211}At$ and Free ^{211}At. The color bar ranges of radioactivity were 0–200 Bq in all images, adding 0–1000 Bq for the top face for clear observation. All four images were almost from black to blue, and little signals were found in Fig. 2. Conversely, some signals were shown on the top face and at the bottom face; specifically, white hole images were found on the top face in Fig. 3, whereas no signals were found at the bottom face. These indicate that there were almost no radio activities on all faces with $Na^{211}At$, whereas some radio activities were detected especially on the top and side faces with Free ^{211}At. We calculated the ratios of the mean activities of each face between $Na^{211}At$ and Free ^{211}At. The ratios of the mean activities of Free ^{211}At were 3.5 times higher than those on the top face, 1.1 times higher than those on the smaller side face, 3.1 times higher than those on the bigger side face, and 1.5 times higher than those at the bottom face in comparison to $Na^{211}At$ on the same faces, respectively. The mean activity of all faces of Free ^{211}At was 2.3 times higher than that of $Na^{211}At$.

The 3D distribution in each radiation source is shown in Fig. 4 ($Na^{211}At$) and Fig. 5 (Free ^{211}At). These images represent 3D distribution quantitatively for each. The 3D distribution of $Na^{211}At$ has more homogeneity than that of Free ^{211}At. The radio activities by ^{211}At were distributed just above the source and the opposite side. Higher activities were shown in the upper area near the top than those at the bottom area. The activities were distributed vertically in both sources and were more widely spread on the opposite side.

Discussion

In this study, we evaluated the 3D distribution of ^{211}At solution dispersion in the small animal cage to simulate the behavior in the lab room. In Japan, the lab room wherein we can use unsealed radioisotopes is strictly managed by the law (Act on Prevention of Radiation Hazards due to Radioisotopes) to prevent radiation hazards due to such activities and to ensure public safety. In addition, research workers who conducted radioisotopes experiment had to follow this law because it provides necessary regulations on the use, dealing, leasing, waste management and other important instructions regarding proper handling of radioisotopes,

Fig. 2

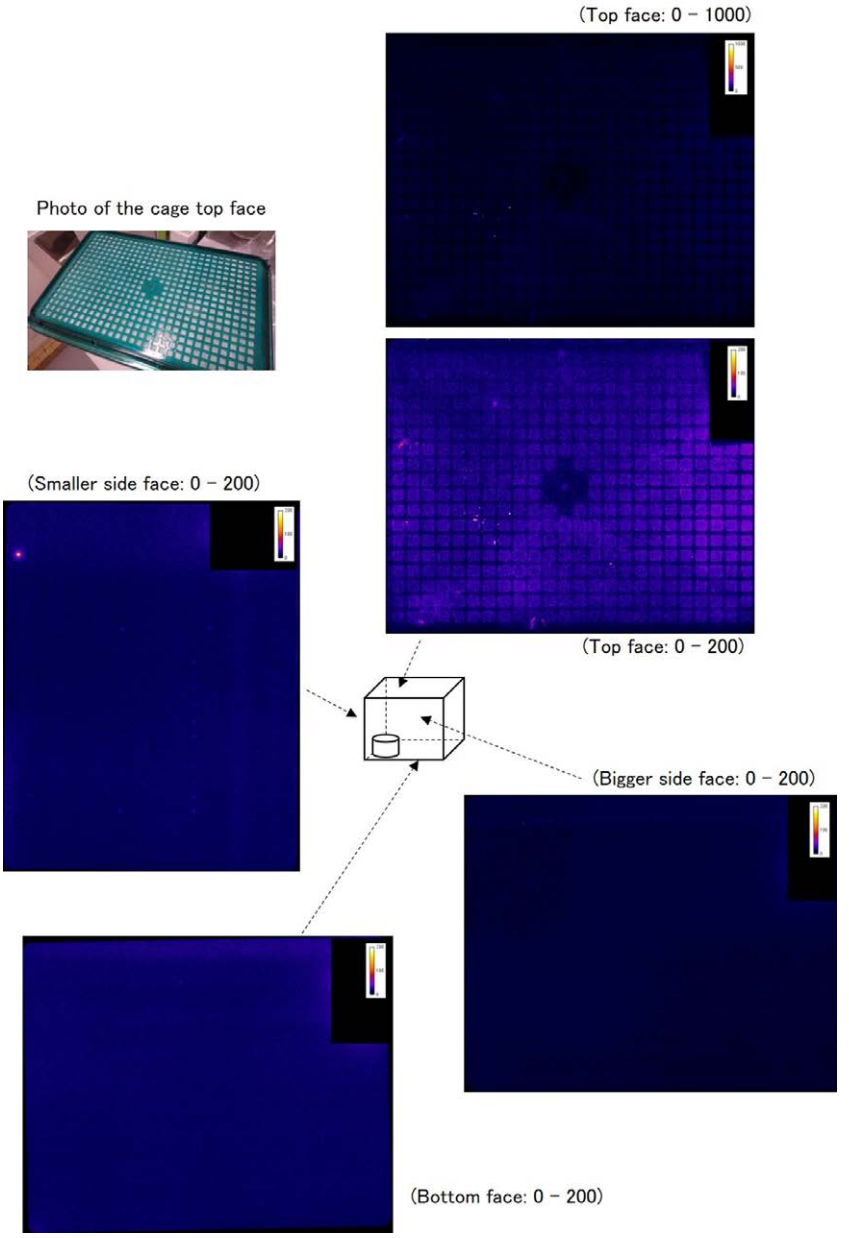

The autoradiography images for four faces of the $Na^{211}At$ source. The range of the radioactivity was adjusted from 0 to 200 Bq, and an image of the top face extended to 1000 Bq was added.

use of radiation generating apparatuses, and handling of objects contaminated with radioisotopes or avoiding radiation emitted from radiation-generating apparatuses.

Following radioisotopes experiment protocols, we also have to keep ourselves from the risk of external radiation and internal exposure. Our assumption that ^{211}At has a risk to vaporize well in the process might have internal exposure to the research workers, but the behavior of ^{211}At in the lab room has not been clear. We aimed to reveal this situation to prevent undesired radiation exposure.

In Japan, the lab room wherein unsealed radioisotopes will be used must have an air conditioning system as required by law. The situation and environment of it resemble the environment of the isolated small animal cage that also has an air conditioning system to control pressure, airflow and air cleanliness. Thus, the combination of an imaging plate and an isolated animal cage was applied to simulate the behavior of ^{211}At solution dispersion. The distribution of the ^{211}At solution was able to be depicted clearly and quantitatively using this combination with a simple experimental

Fig. 3

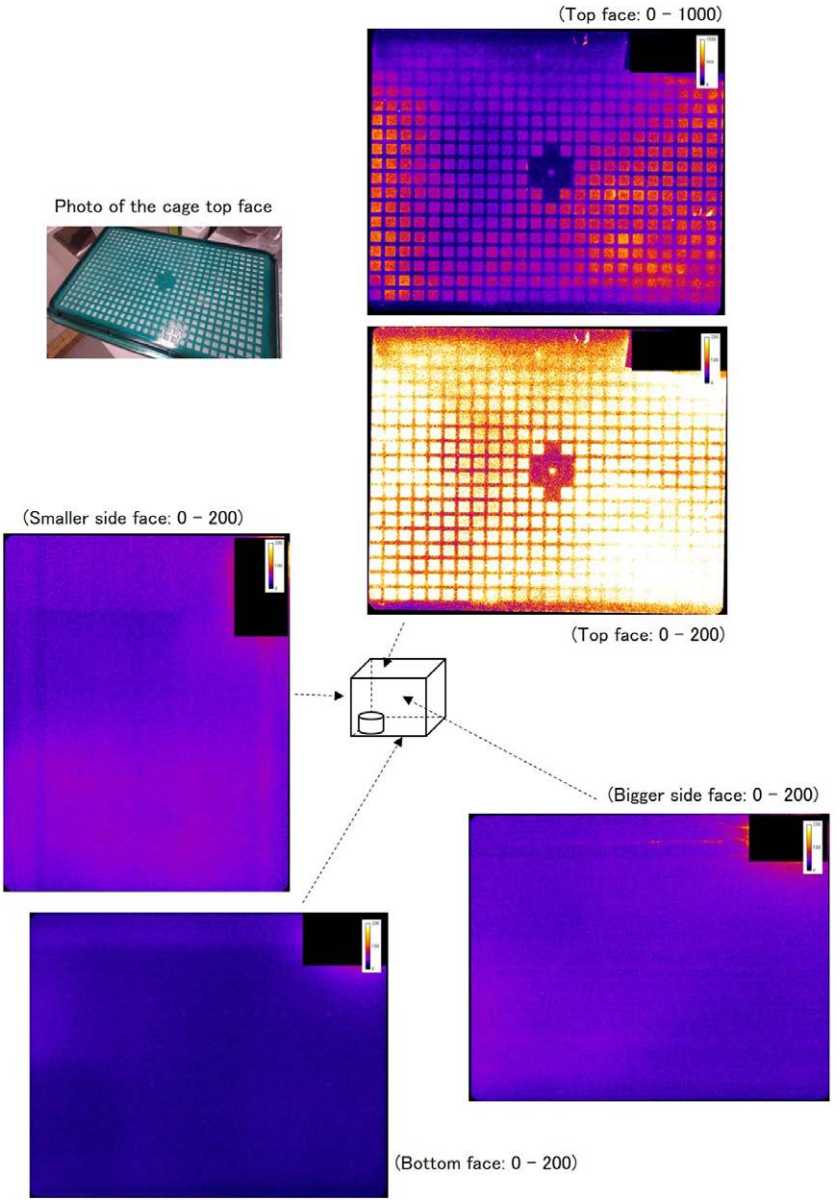

The autoradiography images for four faces of the Free ^{211}At source similar to that in Fig. 2.

method. The total Free ^{211}At activity was approximately twice higher than that of Na^{211}At on autoradiography images. This indicates the volatility of these solutions, and it was shown that Free ^{211}At has high volatility.

In this study, the autoradiography method brought us noticeably clear images that depict the distribution of ^{211}At. The imaging plates that were set on the top face of the cage produced images of the multiple holes of the top cover. These two facts, that is, imaging plate was placed outside of the top face of the cage and multiple holes of the top cover (there is only a filter that was made by nonwoven fabric in these multiple holes), that were depicted show that autoradiography images were produced via the X-ray of EC decay of Po-211 with an energy range of 77–92 keV, not the α-particle from ^{211}At. The previous literature described that ^{211}At decays by a double-branched pathway via 5.87 MeV and 7.45 MeV α-particle emissions [11]. The mean ranges of them in the tissues are approximately 55 and 80 μm, respectively, indicating that the emitted α-particles were not transmitted through the cage walls and top. Another radiation transmitted from ^{211}At is only the K X-rays of the EC decay of Po-211. The same literature described that this X-ray is convenient to count ^{211}At

Fig. 4

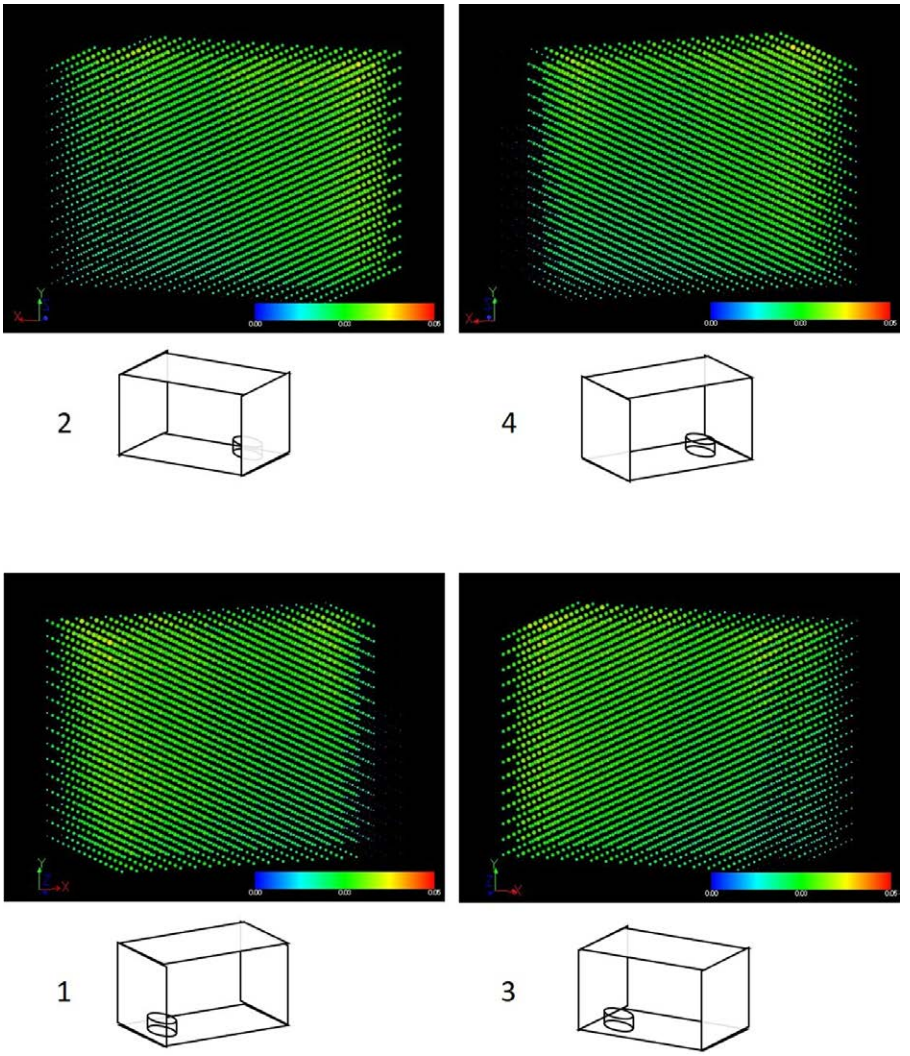

The 3D distribution of $Na^{211}At$ source. Four images with different angles were constructed for clear observation.

activity levels and able to perform scintigraphic imaging of the ^{211}At uptake in the tissues *in vivo*. The material of the cage is polysulfone, with approximately 3-mm thickness. The X-ray absorption calculated on the site [12], having parameters of 1.24 g/cm^3 total density on 77 keV (the lowest X-ray energy) is 0.222 cm^{-1}. From the combination of this X-ray absorption and thickness, the intensity after its cage wall and top transmission is approximately 0.94 of the incident X-ray, suggesting that almost all X-rays passed through the cage walls and top and arrived at the imaging plate. This would indicate that the autoradiography method can be used for evaluating the distribution in the whole cage space in consideration of the X-ray absorption.

In the small cage, the shape of the dispersion of $Na^{211}At$ was almost homogeneous, whereas that of Free ^{211}At was more heterogeneous. Areas directly above and the opposite corners of the source showed much higher activity of ^{211}At. The specification form of the cage describes that the airflow in the cage was laminar, and the velocity was ≤0.15 m/s. The results suggest that vaporized ^{211}At traveled and was stuck to the ceiling of the cage on the contralateral side against the airflow. Although the weight of ^{211}At is just a bit heavier than that of air, it is difficult to understand that ^{211}At traveled in the cage against the airflow. It might be reasonable that some turbulence occurred in the cage and ^{211}At traveled and was stuck with these turbulences. After then, ^{211}At landed at the bottom face owing to its weight. This may indicate the reason for the difference in the activity of the bottom face between both sources. Another possibility is that ^{211}At solutions gathered with micro-dust as a core in the air. The cage system uses a prefilter and high-efficiency particulate air filter to supply air into the cage. It is undeniable that micro-dust was contaminated into the air and can

Fig. 5

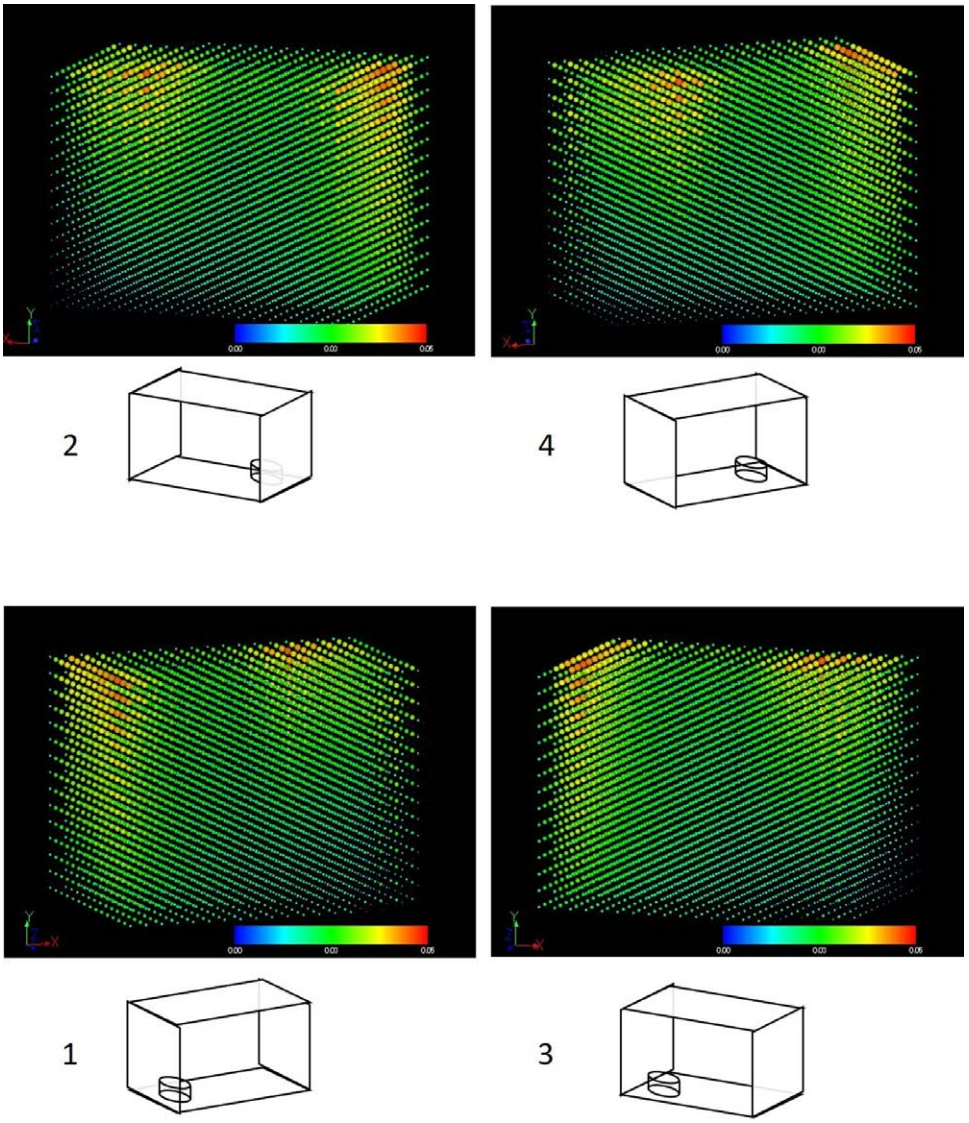

The 3D distribution of Free ^{211}At source similar to that in Fig. 4.

be a core to gather ^{211}At in the air. The mean radioactivity of all the faces of Free ^{211}At was 3.5 times higher than that of Na^{211}At. Some differences in the ratio of mean radioactivity due to the chemical property were observed on each face. This may suggest that ^{211}At vaporized and traveled heterogeneously in the air.

Our findings will contribute in reducing the risks of intake by inhalation or absorption through the skin in the people handling ^{211}At. The highest radioactivity that was measured by imaging plate was less than 1000 Bq, which is relatively low. At this time, the source activity was approximately 100 kBq, while the leaving duration was 3 h. Our findings indicate that the radioactivity hotspot of the vaporized ^{211}At was approximately 1/100 of the original source radioactivity in our experimental environment. From the viewpoint of the clinical situation, our findings will suggest some important points to avoid risks. There is a possibility of hot spot appearances somewhere in a lab room. Its highest activity will be 1/100 of the original source, which will be handled without any shielding. Of course, this was discussed from the viewpoint of the well-tolerated side and ignored or overestimated the room size, chemical form of the source, duration of handling ^{211}At, staying time inside the room, and so on. The kinetics of the vaporized ^{211}At in a lab room is another important issue, which was not evaluated in this study. When we handle ^{211}At, we need enough imagination of the source's spatial and temporal dynamics. Our findings

will be evidence, which would help these imaginations. Evaluating the source's spatial and temporal dynamics should be the next theme.

There are some limitations of study. First, this study was conducted with the assumption that vaporized ^{211}At was suspended in the air and possibly might be stuck after adhesion to the wall. Although we have no evidence for this, ARG images acquired suggested that both phenomena might occur in the cage. Second, we could not evaluate the activities of the source between, before and after placing it in the cage for 3 h. If it were possible to measure it, the vaporized ratio would be evaluated. However, the radioisotopes source was liquid before it turned into polyethylene filter paper, and the liquid was very easy to measure quantitatively. The paper after vaporization was difficult to measure because its sensitivity and quantitative measurement were different from those of the liquid.

We could not reveal the reason why two chemical properties caused differences in the distribution. However, it would be assumed that the vaporized solution had stayed in the air or adhered to the faces of the cage with the differences in the chemical properties. The evidence for the existence of the diatomic astatine (At_2) is sparse and inconclusive. In an aqueous solution, astatine is usually found in the free (0) state [=At(0)], which can be volatilized from the solution. On the contrary, At^- is not volatile, but it may have been oxidized by oxygen in the air and changed to At(0). It is exceedingly difficult for us to identify the cause of these phenomena; we should exercise caution as ^{211}At may travel in the air easily.

Our results show that the 3D dispersion of ^{211}At in the small animal cage was clearly visualized using autoradiography imaging. The 3D distributions of ^{211}At solution dispersion varied in terms of the chemical properties. Our findings can contribute to the evaluation of the behavior of ^{211}At in a lab room with the aim of keeping research workers from the risks of internal exposure and contamination.

Conclusion

We found that the solution of ^{211}At vaporized naturally and was stuck especially at the ceiling and the floor, depending on the environment of the room. We also found that the chemical properties of ^{211}At influenced their behaviors. These results must be considered to minimize the risks of radiation safety when we handle ^{211}At.

Acknowledgements

The authors would like to thank M. Aoki, K. Washiyama, S. Sasaki and K. Nishijima for producing ^{211}At in the cyclotron facility and Enago (www.enago.jp) for the English language review. This work was supported by JSPS KAKENHI Grant Number JP16804878. A part of this work was presented in the 58th annual meeting of the Japanese Society of Nuclear Medicine.

All authors contributed to the study conception and design. Material preparation, data collection and analysis were performed by H.K., S.S. and K.T.. The manuscript's first draft was written by H.K.. All authors commented on the previous versions of the manuscript and read and approved the final manuscript.

Conflicts of interest

There are no conflicts of interest.

References

1 Vaidyanathan G, Zalutsky MR. Applications of 211At and 223Ra in targeted alpha-particle radiotherapy. *Curr Radiopharm* 2011; **4**:283–294.
2 Zalutsky MR, Pruszynski M. Astatine-211: production and availability. *Curr Radiopharm* 2011; **4**:177–185.
3 Guérard F, Gestin JF, Brechbiel MW. Production of [(211)At]-astatinated radiopharmaceuticals and applications in targeted α-particle therapy. *Cancer Biother Radiopharm* 2013; **28**:1–20.
4 Martin TM, Bhakta V, Al-Harbi A, Hackemack M, Tabacaru G, Tribble R, *et al*. Preliminary production of 211At at the Texas A&M University Cyclotron Institute. *Health Phys* 2014; **107**:1–9.
5 Toyoshima A, Nagata K, Ooe K, Zhang Z, Ikeda T, Ichimura S, *et al*. Dispersal rates of astatine-211 from aqueous solutions and chloroform. *Radiat Safety Manag* 2019; **18**:16–22.
6 Lindegren S, Bäck T, Jensen HJ. Dry-distillation of astatine-211 from irradiated bismuth targets: a time-saving procedure with high recovery yields. *Appl Radiat Isot* 2001; **55**:157–160.
7 Spetz J, Rudqvist N, Forssell-Aronsson E. Biodistribution and dosimetry of free 211At, 125I- and 131I- in rats. *Cancer Biother Radiopharm* 2013; **28**:657–664.
8 Watabe T, Kaneda-Nakashima K, Liu Y, Shirakami Y, Ooe K, Toyoshima A, *et al*. Enhancement of 211At uptake via the sodium iodide symporter by the addition of ascorbic acid in targeted α-therapy of thyroid cancer. *J Nucl Med* 2019; **60**:1301–1307.
9 Appelman EH. The oxidation states of astatine in aqueous solution. *J Am Chem Soc* 1961; **83**:805–807.
10 Champion J, Sabatié-Gogova A, Bassal F, Ayed T, Alliot C, Galland N, Montavon G. Investigation of astatine(III) hydrolyzed species: experiments and relativistic calculations. *J Phys Chem A* 2013; **117**:1983–1990.
11 Vaidyanathan G, Zalutsky MR. Astatine radiopharmaceuticals: prospects and problems. *Curr Radiopharm* 2008; **1**:177.
12 Nishikawa Y. Web-based x-ray absorption calculator. Laboratory of Polymer Mechanics, Department of Macromolecular Science and Engineering, Kyoto Institute of Technology. http://www.cis.kit.ac.jp/~kiro/research/kiro. [Accessed 13 February 2021].